Effect of Robertsonian translocations on sperm head form in the house mouse

NURIA MEDARDE[1*], JESSICA MARTÍNEZ-VARGAS[1], ALEJANDRO SÁNCHEZ-CHARDI[2], MARÍA JOSÉ LÓPEZ-FUSTER[3], JACINT VENTURA[1*]

[1]*Departament de Biologia Animal, de Biologia Vegetal i d'Ecologia, Facultat de Biociències, Universitat Autònoma de Barcelona, E-08193 Cerdanyola del Vallès, Spain*

[2]*Servei de Microscopia, Universitat Autònoma de Barcelona, E-08193 Cerdanyola del Vallès, Spain*

[3]*Departament de Biologia Animal and Institut de Recerca de la Biodiversitat (IRBio), Facultat de Biologia, Universitat de Barcelona, E-08007 Barcelona, Spain*

**Corresponding author. E-mail: nuria.estel@gmail.com; jacint.ventura.queija@uab.cat*

Short running title: Sperm head morphology in Rb mice

ABSTRACT

Sperm morphology reflects a long process of adaptation to external conditions and the barriers encountered before ova fertilization can take place; however, not all morphological variation found in gametes can be explained by the effects of these selective forces, as the genetic component may also contribute to the establishment of different gametic features. In north-eastern Spain, there is a wide Robertsonian system of *Mus musculus domesticus*, where individuals with 2*n* ranging from 27 to 40 chromosomes have been described. To elucidate the effect of the karyotype on sperm head form, a comparative analysis between different chromosomal groups of mice from this zone was carried out. Sperm heads from eight St (2*n* = 40) and 24 Rb (2*n* = 30–39) males were processed for scanning electron microscopy and analysed using geometric morphometric techniques. Canonical variate analyses showed substantial shape differences between St and Rb mice in the ventral spur region and between Rb groups in the post-acrosomal region. Significant differences in sperm head size were also detected between chromosomal groups. Structural disorders related to spermatogenesis, genetic alterations, and epistatic interactions among loci are probably involved in the relationship between the phenotypic variation of the sperm head and Rb translocations.

ADDITIONAL KEYWORDS: geometric morphometrics, male gamete, *Mus musculus domesticus*, Robertsonian polymorphism zone, shape, size

INTRODUCTION

The mammalian sperm head is a complex and specialized structure, in which shape and cytoskeletal composition are closely associated with fertilization. Although most eutherian species are characterized by ovoid sperm heads with an apical acrosome and a basal cytoskeleton sheath, in certain species of this group of mammals the sperm head may acquire a higher complexity (Roldan, Gomendio & Vitullo, 1992). Particularly, in most species of the rodent subfamily Murinae, which includes the house mouse (*Mus musculus*), the sperm head is laterally flattened and presents a single hook (Friend, 1936). The nucleus, which occupies most of the head, partially penetrates the hook and gives the head a falciform shape (Lee & Möri, 2006; Avella & Dean, 2011). The acrosomal area, which extends from the convex midedge of the head to the top of the hook, is divided into two parts: the anterior acrosomal region and the equatorial segment (Fig. 1). This first part is mainly composed of enzymatic proteins that are released during the acrosome reaction (Austin & Bishop, 1958; Bedford, 1998; Breed, Idriss & Oko, 2000). The equatorial segment forms a protein–cytoskeletal domain, where the binding of the sperm to the oocyte occurs (Bedford, 1998; Lee & Möri, 2006). Between the nucleus and the acrosome there is a heterogenic cytoskeleton region, the perinuclear theca (Lalli & Clermont, 1981), the protein composition of which varies along the sperm head and is composed of the following structures (Fig. 1): (1) the perforatorium, a cytoskeleton structure found in the apical hook and mainly composed of FABP9/PERF15 perforatorial proteins (Austin & Bishop, 1958; Oko & Clermont, 1988; Bedford, 1998; Breed *et al*., 2000); (2) two ventral spurs, which are rigid extensions located between the flagellum insertion and the apical hook, which have a similar composition to the perforatorium, and are associated with mechanical penetration through the zona pellucida

(Oko & Clermont, 1988); and (3) the post-acrosomal sheath, a structural cytoskeleton lamina that extends beyond the acrosome (Korley, Pouresmaeili & Oko, 1997; Breed *et al*., 2000).

Several studies have revealed that the organization, composition, and function of the sperm head features vary among rodent taxa. This variation can be explained by the effect of sexual forces, such as the animal mating system and postcopulatory sexual selection, which affect sperm morphology in order to achieve fertilization of the ovum (Gomendio & Roldan, 1991; Roldan *et al*., 1992; Breed, 2004, 2005; Malo *et al*., 2006; Martín-Coello *et al*., 2008; Ito *et al*., 2009; Firman, Cheam & Simmons, 2010). However, sexual forces cannot account for all of the variability in sperm form, as genetic variation among individuals (Möri, 1961; Immler, 2008; Turner, Schwahn & Harr, 2011; White *et al*., 2012) may also contribute to the evolution of sperm shape and function.

The western house mouse, *Mus musculus domesticus*, shows an extremely high karyotypic diversity, and is therefore an excellent mammalian model for investigating the effects of chromosomal rearrangements in sperm form. Its standard (St) karyotype consists of 40 acrocentric chromosomes, although the presence of Robertsonian (Rb) fusions leads to a reduction of the diploid number to 22 chromosomes (Piálek, Hauffe & Searle, 2005; Sans-Fuentes *et al*., 2007; Solano, Castiglia & Corti, 2007; Burt, Hauffe & Searle, 2009). A group of populations from a restricted geographical region that share a set of metacentrics with an apparently common evolutionary origin is known as an Rb system (see Piálek *et al*., 2005). In these regions the accumulation of numerous Rb translocations, especially in heterozygous condition, may alter meiotic processes, causing hybrid hypofertility or sterility (Wallace, Searle & Everett, 2002; Merico *et al*., 2003; Manterola *et al*., 2009), and acting as a decisive factor when divergence among populations begins (Hauffe & Searle, 1998). Therefore, inter-

84 individual chromosomal divergence may contribute to the establishment of differences in
85 reproductive success in animals, and variation in gametal traits, such as size and shape, may
86 play an important role at this level.

87 In much of the province of Barcelona and close areas of the provinces of Tarragona and
88 Lleida (northeast Iberian Peninsula) there is a wide Rb polymorphism zone of *M. musculus*
89 *domesticus* (Gündüz *et al*., 2001; Medarde *et al*., 2012). In the 'Barcelona' Rb system
90 (hereafter known as BRbS), Rb animals are bounded by St populations and, to date, no Rb
91 race (*sensu* Hausser *et al*., 1994) has been found (see Medarde *et al*., 2012 and references
92 therein). In the BRbS, diploid numbers range from 27 to 40 chromosomes, and seven
93 different metacentrics (Rb3.8, 4.14, 5.15, 6.10, 7.17, 9.11, and 12.13), which follow a
94 staggered clinal pattern, have been described (Gündüz *et al*., 2001; Sans-Fuentes *et al*., 2007;
95 Medarde *et al*., 2012). Morphological and ethological studies in mice from this zone have
96 revealed that Rb translocations are involved in the decreased gene flow between
97 karyotypically differentiated populations (Muñoz-Muñoz *et al*., 2003, 2006, 2011; Sans-
98 Fuentes *et al*., 2005, 2009). These findings, together with alterations in the spermatogenesis
99 found in Rb mice (Sans-Fuentes *et al*., 2010), led us to hypothesize that the Rb fusions might
100 have an impact on sensitive systems, such as the gametes, and thus promote shape changes
101 in the sperm features. This hypothesis is supported by the results obtained in laboratory
102 crosses between different lineages of *M. musculus*, which demonstrated that sperm
103 morphology is severely influenced by changes in loci linked to specific chromosomes (Oka *et*
104 *al*., 2007; White *et al*., 2012).

105 The main aim of this study was to ascertain the effect, if any, of the diploid number and
106 structural composition of the karyotype on the form (size and shape) of the sperm head in

specimens of *M. musculus domesticus* from the BRbS. To this end, comparative analyses between St and different groups of Rb mice were undertaken by applying geometric morphometric (GM) techniques on landmark data obtained from scanning electron microscopy (SEM) images. To our knowledge, this is the first attempt to determine the possible relationships between this type of chromosomal rearrangement and sperm head form.

MATERIAL AND METHODS

Epididymal samples obtained from 32 mature males from the BRbS were used to analyse the variation in sperm head morphology (Table 1). From each specimen, the left cauda epididymis was dissected and disaggregated in 5 mL of phosphate buffer (PB 0.1 M) at room temperature (23 ºC). After homogenization, 1 mL of sperm solution was filtered through a Nucleopore membrane (0.2 µm) and immediately fixed overnight in a solution of 2.5% glutaraldehyde, 2% paraformaldehyde, and PB 0.1 M solution at 4 °C. The samples were then rinsed in PB 0.1 M, postfixed in 1% osmium tetroxide, rinsed in PB 0.1 M, dehydrated in a graded series of ethanol, and dried using the critical-point method. Membranes were mounted on stubs, coated with gold, and observed in an S-570 scanning electron microscope (Hitachi, Japan) operating at an accelerating voltage of 15 kV. From each left cauda epididymis, an average of 20 sperm heads in a horizontal plane, with the hook orientated to the left-hand side and without any evident alterations to the structure (e.g. absence of hook, bent neck, or double headed), were randomly captured (Fig. 1).

Taking into account previous results regarding the phenotypic relationships between different chromosomal groups in the BRbS (see Muñoz-Muñoz *et al*., 2003, 2006, 2011; Sans-

Fuentes *et al*., 2009), specimens were assigned to the following categories: St, specimens with all acrocentric chromosomes (2*n* = 40); Rb(38–40), animals with one or two Rb translocations and specimens with all acrocentric chromosomes collected in sites with Rb mice; Rb(33–37), individuals with between three and seven Rb fusions; and Rb(30–32), mice with between eight and ten Rb fusions. In order to study the effects of the structural composition of the karyotype (Ht), the specimens were pooled as follows: AA, individuals with all acrocentric chromosomes; Ht, specimens with between one and three heterozygous fusions; and MM, mice with homozygous fusions only. Note that Ht specimens may have heterozygous translocations alone or combined with between one and four fusions in homozygous state. Karyotypes were determined from bone marrow plates (Ford, 1966) and stained using Wright Staining for G bands (Mandahl, 1992). Chromosomes were identified under a light microscope according to the Committee on Standarized Genetic Nomenclature for Mice (1972).

Morphometric analyses were performed using the tps series by Rohlf (2006) and the MorphoJ software package (Klingenberg, 2011). Sixteen twodimensional landmarks and three semilandmarks were digitized around each sperm head using tpsDig2 software (Fig. 1). Semilandmarks (points 16–18), which correspond to the curved contour of the acrosomal region, were digitized as equidistant points using the tool ‘draw background curves’ and the option ‘resample curve by length’ in tpsDig2.

As the first analyses revealed variations in sperm width among the Rb groups (see Results), a sperm subsample of extreme Rb animals was also analysed using conventional light microscopy (LM) techniques to ensure that shape variations were not affected by the SEM procedure. Thus, following the measurement points defined by Braden (1958), the length

and width of 20 sperm heads from five Rb(38–40) and five Rb(30–32) mice were recorded using tpsDig2. This procedure was also applied for SEM images. The mean of each parameter was obtained for each individual. Differences among groups were tested by Student's *t*-test. To evaluate the bias between the two methods, Pearson's correlation test, Bland–Altman plot, and Passing–Bablok regression analysis were applied to the width and length measurements.

Landmark and semilandmark configurations of all sperm heads were superimposed using Procrustes analysis in order to obtain the size and shape variables (Rohlf & Slice, 1990). Size was defined as centroid size (CS; see Bookstein, 1991). Allometry, assumed as size-dependent shape variation, was tested in the whole sample and in each chromosomal group by means of a multivariate analysis of covariance (MANCOVA), with CS as the covariate, and a linear multivariate regression of the Procrustes coordinates on the CS (MorphoJ 1.04b). The statistical significance of the allometric regressions was calculated by a permutation test with 10 000 iterations, under the null hypothesis of independence between size and shape, by randomly exchanging the value for CS among individuals (Good, 1994). Given that a significant dependence of shape on size was detected (see Results), the residuals obtained in the multivariate regression analyses were used for subsequent analyses (Frost *et al*., 2003).

A nested ANOVA was performed to separate intra and inter-individual variation in both the size and shape of the sperm head (MorphoJ 1.04b). To test for shape differences between chromosomal groups, a canonical variate analysis (CVA) was performed. Transformation grids were used to visualize shape variations indicated by the first two canonical axes (MorphoJ 1.04b). Mahalanobis distances were obtained to assess statistically significant differences between groups (Table 2). A multivariate analysis of variance (MANOVA) was applied to all

canonical vectors (CVs) to estimate the effect of 2*n* and Ht on sperm shape variation. Differences in size associated with 2*n* and Ht were tested with one-way and twoway analyses of variance (ANOVA) applied to CS. A Tukey's post-hoc test was performed to evaluate differences in CS between pairs of chromosomal groups. All statistical analyses were performed with STATISTICA 8.0.

Permission to capture was granted by the Departament de Medi Ambient of the Generaltitat de Catalunya (Spain). Animals were handled in compliance with the guidelines and ethical approval of the Comissió d'Ètica en l'Experimentación Animal y Humana of the Universitat Autònoma de Barcelona and by the Departament d'Agricultura, Ramaderia, Pesca, Alimentació i Medi Natural of the Generalitat de Catalunya (reference of the experimental procedure authorization: DAAM 6328).

RESULTS

Comparison of the morphometric results obtained by light and electron microscopy revealed significantly lower values in the length and width of the sperm heads treated with SEM ($P < 0.05$); however, the accuracy of the measurements obtained from the SEM images was higher than those corresponding to LM (see Appendix S1). Both methods showed a strong correlation in the morphological variation pattern detected in the samples (sperm head length, $r = 0.65$; sperm head width = 0.67; in both parameters, $P < 0.001$; see Appendix S2), which supports the differences observed in the size and narrowing of the sperm head among Rb(38–40) and Rb(30–32) groups in the GM analyses (see below). Passing–Bablok regression analysis also indicated good agreement between the SEM and LM methods, with no systematic or proportional differences between them ($P > 0.1$ for both sperm width and

length). Bland–Altman analysis showed that, despite the sample shrinkage related to the SEM treatment, there was high concordance between both methods (see Appendix S2).

Using the whole sample, MANCOVA with CS as a covariate revealed a significant relationship between the shape and size of the sperm head ($F = 5.13$, d.f. = 102, $P < 0.001$). Multivariate regression between shape and size variables predicted close to 10% allometry for both 2*n* and Ht groups (10.07 and 9.79%, respectively; $P < 0.001$ in both cases).

The nested ANOVA indicated that phenotypic variation within individuals was lower than that found between individuals from the same chromosomal group (shape, MSwithin individuals = 0.0273, MSamong groups = 0.0752; CS, MSwithin individuals = 0.9231; MSamong groups = 1.9713; $P < 0.001$ in both cases). For 2*n* groups, CVA provided three functions that correctly classified 70.3% of the sperm. The first (CV1) and second (CV2) axes accounted for 89.88% of the total variation between groups (Fig. 2). Shape changes along CV1 (69.01% of the variation) were related to the distance between the ventral spurs. This axis clearly separated the sperm heads of St animals from those corresponding to the other mice groups. Deformation grids on CV1 showed that the sperm head in St mice generally showed an upward movement of landmarks 4 and 5, which produce a relative shortening of the upper ventral spur and an increased distance between the upper and the lower spurs. This shape modification (Fig. 3) was associated with small changes in the perforatorium (landmarks 1 and 19) and the postacrosomal sheath (landmarks 12 and 13). The main shape variation along CV2 (20.87%) was related to the width of the post-acrosomal region of the sperm head. This axis allowed a certain separation between Rb(38–40) and the other 2*n* groups. Deformation grids on CV2 showed that the sperm head of Rb(38–40) specimens tended to be narrower than the rest of the samples (Fig. 3), indicating the retraction of the

apical process and anterior acrosomal region (landmarks 1–15) and of the post-acrosomal region associated with the flagellum (landmarks 10–12). Mahalanobis distances revealed significant differences between chromosomal groups (Table 2).

Analysis computed for Ht provided two functions, which correctly separated 79.9% of the sperm heads. The CV1 explained 75.3% of the total variation and shape changes in the canonical space revealed a similar trend to that obtained for 2*n* analysis, although differences among the groups were less appreciable (Appendix S3).

A MANOVA applied on CVs revealed a significant effect of 2*n* ($F2n = 151.08$, d.f. = 9, $P < 0.001$), Ht ($F\text{Ht} = 61.86$, d.f. = 6, $P < 0.001$), and their interaction ($F2n*\text{Ht} = 3.54$, d.f. = 3, $P = 0.015$) on sperm head shape, which also suggests substantial differences among the St and Rb sperm. For each Rb sample, shape traits varied unequally depending on the balance between the number of Rb fusions and the structural composition of the karyotype (Fig. 4). In CV1 a noticeable separation between St and the other chromosomal groups was detected; along CV2 Rb(38–40) animals appeared clearly separated from the rest of Rb specimens, with St mice placed in an intermediate position but close to the homozygous groups (Fig. 4). Two-way ANOVAs showed significant differences in CS among groups ($F2n*\text{Ht} = 13.29$, d.f. = 1, $P = 0.003$). Likewise, one-way ANOVA revealed significant differences relating to each factor ($F2n = 12.92$, d.f. = 3, $P < 0.001$; $F\text{Ht} = 11.77$, d.f. = 2, $P < 0.001$). Consistent with the shape analysis, sperm head size exhibited different variation patterns in terms of chromosomal polymorphism and structural composition of the karyotype. In general, the sperm head was larger in animals with the lowest diploid number [Rb(30–32)] and fusions in the heterozygous state; however, within this Rb group, mice with all fusions in homozygous condition showed the smallest mean values of CS of the whole sample

(Fig. 5). Both Rb(30–32) groups differed significantly in sperm head size with respect to most chromosomal groups (Table 3).

DISCUSSION

The high resolution of SEM images and accuracy in form analysis offered by GM techniques provided a more detailed and precise method for evaluating sperm head morphological features than conventional LM methods. GM is a sensitive technique that allows the detection of subtle shape changes. Hence, differences in the position of the structures compared in the horizontal plane, or the low resolution of images, could produce an overestimation of the results. Moreover, the SEM method facilitates the observation of several structures (such as the edges of the equatorial segment and the anterior acrosomal region, the tops of the post-acrosomal region, and the ventral spurs) that could be underestimated by LM, thereby inducing a lack of precision in landmark location. Although SEM treatment may involve a slight decrease in sperm size, probably because of membrane shrinkage during the sample dehydration process, our morphometric analyses strongly correlate with the morphological differences detected using LM. Additionally, as all samples were processed using the same procedure, we can expect no bias in the results from SEM treatment.

The results of this study reveal a substantial variation in the size and shape of the sperm head in *M. musculus domesticus* in relation to karyotypic configuration. It has been reported that Rb translocations lead to the loss of telomeric and minor satellite DNA sequences from the acrocentric chromosomes involved in these rearrangements (Garagna *et al*., 1995, 2001). Additionally, these mutations affect the rates and patterns of chromosomal recombination,

varying the number and distribution of genic exchanges in the metacentric chromosomes (Rieseberg, 2001; Dumas & Britton-Davidian, 2002) and modifying the genetic linkage groups (Davison & Akeson, 1993; Rieseberg, 2001). Accordingly, the expression and regulation patterns of several genes involved in sperm morphogenesis might be altered when Rb translocations are present (Eaker *et al*., 2001; Merico *et al*., 2003, 2008; Manterola *et al*., 2009), and these probably affect mature sperm head features. Concordantly, certain studies have demonstrated an association between alterations in particular loci and changes in sperm phenotype. Thus, for example, results obtained from laboratory crosses between different lineages of *M. musculus* demonstrated that sperm head morphological variation is associated with loci in chromosomes Y (Styrna, Klag & Moriwaki, 1991; Styrna & Krzanowska, 1995; Styrna, Bilin´ ska & Krzanowskaa, 2002), 11 (Oka *et al*., 2007), 7, and X (White *et al*., 2012). Likewise, it has been shown that epistatic interactions can significantly alter the sperm head phenotype in an additive manner: for example, hybridizations between *M. musculus musculus* and *M. musculus domesticus* revealed that certain pairs of loci (in chromosomes 4 and X, 11 and X, and X and X) affected sperm head morphology (White *et al*., 2012). All these findings suggest that the relationship between Rb fusions and the phenotypic variation in the sperm head detected in the present study has a complex genetic basis, with epistatic interactions playing a relevant role.

Morphometric analyses reveal that the greatest shape variation between St and Rb groups occurred in the ventral spurs. Specifically, mice with metacentric chromosomes showed smaller spurs, which, in turn, are closer to each other. As reported for other Murinae, such as *Apodemus agrarius* (Lee & Möri, 2006), *Aethomys chrysophilus* (Breed *et al*., 2000), and *Rattus norvegicus* (Oko & Clermont, 1988), the ventral spurs in *M. musculus domesticus* consist of a rigid extension of sperm head cytoskeleton, and are mainly composed of the

male germ cell-specific fatty acid-binding protein FABP9/PERF15 (Oko & Morales, 1994; Korley *et al*., 1997). Phenotypic studies in laboratory mouse strains revealed a close relationship between levels of FABP9/PERF15 and ventral spur development, so mice lacking from this protein showed a reduction or an absence of these structures in a moderate number of sperm heads (Farkhondeh *et al*., 2009; Selvaraj *et al*., 2010). Thus, variations in ventral spur morphology might be related to genetic factors involved in the synthesis of such protein. Accordingly, it cannot be ruled out that the Rb fusions might have some effect on the expression of FABP9/PERF15 and consequently on the phenotype of the ventral spurs in Rb animals.

In addition to the shape differences in the ventral spur region between Rb and St mice, Procrustes analyses also revealed different narrowing profiles between chromosomal groups. Specifically, whereas sperm heads in animals belonging to the Rb(38–40) group showed the narrowest post-acrosomal region, the widest sperm heads were found in mice with a higher number of translocations [Rb(30–32) and Rb(33–37)]. Sperm of St animals generally showed intermediate shapes. Spermatid elongation is a process partially controlled by sperm gene expression (Johnson, 2007). In this process, the synthesis of proteins involved in nuclear compaction, and/or in the assemblage of microtubular structures that lead to acrosomal and nuclear elongation (such as the acroplaxome or the perinuclear ring), is essential for producing viable gametes (Lalli & Clermont, 1981; Toshimori & Ito, 2003). Our results indicate that changes in the sperm differentiation process can be promoted by Rb translocations; however, the great morphological variation detected among Rb groups suggests that other factors, such as the number of fusions or the structural composition of the karyotype, can play a relevant role during the sperm cytodifferentiation process.

As regards to sperm head size, our results revealed that Rb(30–32) mice with structural heterozygosis showed the highest mean CS values, whereas the smallest values corresponded to the homozygotes of the Rb(30–32) and Rb(33–37) groups. This pattern is generally consistent with the shape differences between Rb groups, in terms of sperm head width, so the increased sperm head size is related to stretching. This suggests that the presence of a relatively high number of fusions in the homozygous condition combined with heterozygous metacentric chromosomes might complicate the nuclear compaction process, altering the spermatid elongation. In such a scenario, it would be interesting to know the possible relationships between the shape of the sperm nucleus and the sperm head shape. Nevertheless, other factors, such as flagellum length, may also be involved in sperm head size differences between chromosomal groups. Comparative analyses on closely related Muridae species showed that an increase in one sperm component, for example the sperm head, is accompanied by an increase in other sperm structures such as the midpiece and the flagellum (Gómez-Montoto *et al*., 2011). Additionally, the total length of the spermatozoa is strongly associated with the sperm's swimming velocity, which in turn is highly related to sperm competition levels (Gomendio & Roldan, 2008; Gómez-Montoto *et al*., 2011). Although analysis of the size of the midpiece and flagellum would be beyond the scope of this study, and nothing is known regarding the reproduction potential and fertility of the different chromosomal groups studied here, background information on interespecific comparisons allow us to hypothesize that the decrease in sperm head size found in Rb homozygotes with a relatively high number of fusions also entails a shortening of the flagellum and, consequently, a decrease in the swimming velocity of the sperm. It is clear that analyses that reveal the relationships between sperm size, sperm number, and sperm quality in Rb systems of *M. musculus domesticus* would provide crucial insights into this

subject. Likewise, further morphological and functional analyses on sperm cells, together with breeding studies under controlled conditions, are needed to elucidate the extent to which reproductive fitness is altered in Rb mice.

ACKNOWLEDGEMENTS

We thank Francesc Muñoz for statistical assistance and Josep Medarde for his help with the fieldwork. This article was improved by comments from William G. Breed and two anonymous reviewers. This study was funded by the Spanish Ministerio de Economía y Competitividad (project number CGL2010-15243) and by a PIF (Personal Investigador en Formació) grant from the Universitat Autònoma de Barcelona to N.M.

REFERENCES

Austin CR, Bishop MWH. 1958. Some features of the acrosome and perforatorium in mammalian spermatozoa. *Proceedings of the Royal Society of London. Series B, Biological Sciences* **149:** 234–240.

Avella MA, Dean J. 2011. Fertilization with acrosomereacted mouse sperm: implications for the site of exocytosis. *Proceedings of the National Academy of Sciences of the United States of America* **50:** 19843–19844.

Bedford JM. 1998. Mammalian fertilization misread? Sperm penetration of the eutherian zona pellucida is unlikely to be a lytic event. *Biology of Reproduction* **59:** 1275–1287.

Bookstein FL. 1991. *Morphometric tools for landmark data: geometry and biology*. Cambridge: Cambridge University Press.

Braden AWH. 1958. Strain differences in the morphology of the gametes of the mouse. *Australian Journal of Biological Sciences* **12:** 65–71.

Breed WG. 2004. The spermatozoon of eurasian murine rodents: its morphological diversity & evolution. *Journal of Morphology* **261:** 52–69.

Breed WG. 2005. Evolution of the spermatozoon in muroid rodents. *Journal of Morphology* **265:** 271–290.

Breed WG, Idriss D, Oko RJ. 2000. Protein composition of the ventral processes on the sperm head of Australian hydromyine rodents. *Biology of Reproduction* **63:** 629–634.

Burt G, Hauffe HC, Searle JB. 2009. New metacentric population of the house mouse (*Mus musculus domesticus*) found in Valchiavenna, northern Italy. *Cytogenetic and Genome Research* **125:** 260–265.

Committee on Standarized Genetic Nomenclature for Mice. 1972. Standard karyotype of the mouse, *Mus musculus*. *Heredity* **63:** 69–72.

Davison MT, Akeson EC. 1993. Recombination suppression by heterozygous Robertsonian chromosomes in the mouse. *Genetics* **133:** 649–667.

Dumas D, Britton-Davidian J. 2002. Chromosomal rearrangements and evolution of recombination: comparison of chiasma distribution patterns in standard and Robertsonian populations of the house mouse. *Genetics* **162:** 1355–1366.

Eaker S, Pyle A, Cobb J, Handel MA. 2001. Evidence for meiotic spindle checkpoint from analysis of spermatocytes from Robertsonian-chromosome heterozygous mice. *Journal of Cell Science* **114:** 2953–2965.

Farkhondeh P, Tahereh K, Mahmood JT, Mojgan B, Jamileh G, Fatemeh SN. 2009. A novel human lipid binding protein coding gene: PERF15, sequence and cloning. *Journal of Reproduction and Infertility* **10:** 199–205.

385 **Firman RC, Cheam LY, Simmons LW. 2010.** Sperm competition does not influence sperm
386 hook morphology in selection lines of house mice. *Journal of Evolutionary Biology* **24:**
387 856–862.
388 **Ford CE. 1966.** The use of chromosome markers. In: Micklem HS, Loutit JF, eds. *Tissue*
389 *grafting and radiation*. New York: Academic Press, 197–206.
390 **Friend GF. 1936.** The sperms of British muridae. *The Quarterly Journal of Microscopical*
391 *Science* **78:** 419–443.
392 **Frost SR, Marcus LF, Bookstein FL, Reddy DP, Delson E. 2003.** Cranial allometry,
393 phylogeography, and systematics of large-bodied papionins (Primates: Cercopithecinae)
394 inferred from geometric morphometric analysis of landmark data. *The Anatomical Record.*
395 *Part A, Discoveries in Molecular, Cellular, and Evolutionary Biology* **275:** 1048–1072.
396 **Garagna S, Broccoli D, Redi CA, Searle JB, Cooke HJ, Capanna E. 1995.** Robertsonian
397 metacentrics of the house mouse lose telomeric sequences but retain some minor
398 satellite DNA in the pericentromeric area. *Chromosoma* **103:** 685–692.
399 **Garagna S, Marziliano N, Zuccotti M, Searle JB, Capanna E, Redi CE. 2001.** Pericentromeric
400 organization at the fusion point of mouse Robertsonian translocation chromosomes.
401 *Proceedings of the National Academy of Sciences of the United States of America* **98:** 171–
402 175.
403 **Gomendio M, Roldan ERS. 1991.** Sperm competition influences sperm size in mammals.
404 *Proceedings of the Royal Society of London. Series B, Biological Sciences* **243:** 181–185.
405 **Gomendio M, Roldan ERS. 2008.** Implications of diversity in sperm size and function for
406 sperm competition and fertility. *The International Journal of Developmental Biology* **52:**
407 439–447.

Gómez-Montoto L, Varea-Sánchez M, Tourmente M, Martín-Coello J, Luque-Larena JJ, Gomendio M, Roldan ERS. 2011. Sperm competition differentially affects swimming velocity and size of spermatozoa from closely related muroid rodents: head first. *Reproduction* **142:** 819–830.

Good P. 1994. *Permutation tests: a practical guide to resampling methods for testing hypotheses*. New York: Springer-Verlag.

Gündüz I, López-Fuster MJ, Ventura J, Searle JB. 2001. Clinal analysis of a chromosomal hybrid zone in the house mouse. *Genetical Research* **77:** 41–51.

Hauffe HC, Searle JB. 1998. Chromosomal heterozygosity and fertility in house mice (*Mus musculus domesticus*) from northern Italy. *Genetics* **150:** 1143–1154.

Hausser J, Fedyk S, Fredga K, Searle JB, Volobouev V, Wójcik JM, Zima J. 1994. Definition and nomenclature of the chromosome races of *Sorex araneus*. *Folia Zoologica* **43:**1–9.

Immler S. 2008. Sperm competition and sperm cooperation: the potential role of diploid and haploid expression. *Reproduction* **135:** 275–283.

Ito C, Akutsu H, Yao R, Kyono K, Suzuki-Toyota F, Toyama Y, Maekawa M, Noda T, Toshimori K. 2009. Oocyte activation ability correlates with head flatness and presence of perinuclear theca substance in human and mouse sperm. *Human Reproduction* **24:** 2588–2595.

Johnson MH. 2007. *Essential reproduction, 6th edn*. Cambridge: Blackwell Publishing. University of Cambridge.

Klingenberg CP. 2011. MorphoJ: an integrated software package for geometric morphometrics. *Molecular Ecology Resources* **11:** 353–357.

Korley R, Pouresmaeili F, Oko R. 1997. Analysis of the protein composition of the mouse sperm perinuclear theca and characterization of its major protein constituent. *Biology of Reproduction* **57:** 1426–1432.

Lalli M, Clermont Y. 1981. Structural changes of the head components of the rat spermatid during late spermiogenesis. *The American Journal of Anatomy* **160:** 419–434.

Lee JH, Möri T. 2006. Ultrastructural observations on the sperm of two *Apodemus* species, *Apodemus agrarius coreae* and *Apodemus speciosus peninsulae*, in Korea. *Journal of the Faculty of Agriculture – Kyushu University* **51:** 125– 133.

Malo AF, Gomendio M, Garde J, Lang-Lenton B, Soler AJ, Roldan ERS. 2006. Sperm design and sperm function. *Biology Letters* **2:** 246–249.

Mandahl N. 1992. Methods in solid tumour cytogenetics. In: Rooney DE, Czepulkowski BH, eds. *Human cytogenetics. A practical approach*. London: IRL Press, 155–187.

Manterola M, Page J, Vasco C, Berríos S, Parra MT, Viera A, Rufas JS, Zuccotti M, Garagna S, Fernández-Donoso R. 2009. A high incidence of meiotic silencing of unsynapsed chromatin is not associated with substantial pachytene loss in heterozygous male mice carrying multiple simple Robertsonian translocations. *PLoS Genetics* **5:** e1000625.

Martín-Coello J, Benavent-Corai J, Roldan ERS, Gomendio M. 2008. Sperm competition promotes asymmetries in reproductive barriers between closely related species. *Evolution* **63:** 613–623.

Medarde N, López-Fuster MJ, Muñoz-Muñoz F, Ventura J. 2012. Spatio-temporal variation in the structure of a chromosomal polymorphism zone in the house mouse. *Heredity* **109:** 78–89.

Merico V, Diaz de Barbosa G, Vasco C, Ponce R, Rodriguez V, Garagna S, Tolosa de Talamoni N. 2008. A mitochondrial mechanism is involved in apoptosis of Robertsonian mouse male germ cells. *Reproduction* **135:** 797–804.

Merico V, Pigozzi MI, Esposito A, Merani MS, Garagna S. 2003. Meiotic recombination and spermatogenic impairment in *Mus musculus domesticus* carrying multiple simple Robertsonian translocations. *Cytogenetic and Genome Research* **103:** 321–329.

Möri A. 1961. The difference in sperm-morphology in different strains of mice. *Tohoku Journal of Agricultural Research* **12:** 107–118.

Muñoz-Muñoz F, Sans-Fuentes MA, López-Fuster MJ, Ventura J. 2003. Non-metric morphological divergence in the western house mouse, *Mus musculus domesticus*, from the Barcelona chromosomal hybrid zone. *Biological Journal of the Linnean Society* **80:** 313–322.

Muñoz-Muñoz F, Sans-Fuentes MA, López-Fuster MJ, Ventura J. 2006. Variation in fluctuating asymmetry levels across a Robertsonian polymorphic zone of the house mouse. *Journal of Zoological Systematics and Evolutionary Research* **44:** 236–250.

Muñoz-Muñoz F, Sans-Fuentes MA, López-Fuster MJ, Ventura J. 2011. Evolutionary modularity of the mouse mandible: dissecting the effect of chromosomal reorganizations and isolation by distance in a Robertsonian system of *Mus musculus domesticus*. *Journal of Evolutionary Biology* **24:** 1763–1776.

Oka A, Aoto T, Totsuka Y, Takahashi R, Ueda M, Mita A, Sakurai-Yamatani N, Yamamoto H, Kuriki S, Takagi N, Moriwaki K, Shiroishi T. 2007. Disruption of genetic interaction between two autosomal regions and the X chromosome causes reproductive isolation between mouse strains derived from different subspecies. *Genetics* **175:** 185–197.

475 **Oko R, Clermont Y. 1988.** Isolation, structure and protein composition of the perforatorium
476 of rat spermatozoa. *Biology of Reproduction* **39:** 673–687.
477 **Oko R, Morales CR. 1994.** A novel testicular protein, with sequence similarities to a family of
478 lipid binding proteins, is a major component of the rat sperm perinuclear theca.
479 *Developmental Biology* **166:** 235–245.
480 **Piálek J, Hauffe HC, Searle JB. 2005.** Chromosomal variation in the house mouse. *Biological*
481 *Journal of the Linnean Society* **84:** 535–563.
482 **Rieseberg L. 2001.** Chromosomal rearrangements and speciation. *Trends in Ecology &*
483 *Evolution (Personal edition)* **16:** 351–358.
484 **Rohlf FJ. 2006.** *Tps software*. *TpsDig2, version 2.16.* Department of Ecology and Evolution,
485 State University of New York at Stony Brook, Available at:
486 http://life.bio.sunysb.edu/morph/
487 **Rohlf JM, Slice DE. 1990.** Extensions of the Procrustes method for the optimal
488 superimposition of landmarks. *Systematic Zoology* **39:** 40–59.
489 **Roldan ERS, Gomendio M, Vitullo D. 1992.** The evolution of eutherian spermatozoa and
490 underlying selective forces: female selection and sperm competition. *Biological Reviews*
491 **67:** 551–593.
492 **Sans-Fuentes MA, García-Valero J, Ventura J, López-Fuster MJ. 2010.** Spermatogenesis in
493 house mouse in a Robertsonian polymorphism zone. *Reproduction* **140:** 560–581.
494 **Sans-Fuentes MA, López-Fuster MJ, Ventura J, Diez-Noguera A, Cambras T. 2005.** Effect of
495 Robertsonian translocations on circadian rhythm of motor activity in house mouse.
496 *Behavior Genetics* **35:** 603–613.

Sans-Fuentes MA, Muñoz-Muñoz F, Ventura J, López-Fuster MJ. 2007. Rb(7.17), a rare Robertsonian fusion in wild populations of the house mouse. *Genetical Research* **89:** 207–213.

Sans-Fuentes MA, Ventura J, López-Fuster MJ, Corti M. 2009. Morphological variation in house mice from the Robertsonian polymorphism area of Barcelona. *Biological Journal of the Linnean Society* **97:** 555–570.

Selvaraj V, Asano A, Page JL, Nelson JL, Kothapalli KS, Foster JA, Brenna JT, Weiss RS, Travis AJ. 2010. Mice lacking FABP9/PERF15 develop sperm head abnormalities but are fertile. *Developmental Biology* **348:** 177–189.

Solano E, Castiglia R, Corti M. 2007. A new chromosomal race of the house mouse, *Mus musculus domesticus*, in the Vulcano Island-Aeolian Archipelago, Italy. *Hereditas* **144:** 75–77.

Styrna J, Bilińska B, Krzanowskaa H. 2002. The effect of a partial Y chromosome deletion in B10.BR-Ydel mice on testis morphology, sperm quality and efficiency of fertilization. *Reproduction, Fertility, and Development* **14:** 101–108.

Styrna J, Klag J, Moriwaki K. 1991. Influence of partial deletion of the Y chromosome on mouse sperm phenotype. *Journal of Reproduction and Fertility* **92:** 187–195.

Styrna J, Krzanowska H. 1995. Sperm select penetration test reveals differences in sperm quality in strains with different Y chromosome genotype in mice. *Archives of Andrology* **35:** 111–118.

Toshimori K, Ito C. 2003. Formation and organization of the mammalian sperm head. *Archives of Histology and Cytology* **66:** 383–396.

Turner LM, Schwahn DJ, Harr B. 2011. Reduced male fertility is common but highly variable in form and severity in a natural house mouse hybrid zone. *Evolution* **66:** 443–458.

Wallace BM, Searle JB, Everett CA. 2002. The effect of multiple simple Robertsonian heterozygosity on chromosome pairing and fertility of wild-stock house mice (*Mus musculus domesticus*). *Cytogenetic and Genome Research* **96:** 276–286.

White MA, Stubbings M, Dumont BL, Payseur BA. 2012. Genetics and evolution of hybrid male sterility in house mice. *Genetics* **191:** 917–934.

TABLES

Table 1. Collection sites and individual karyotypes of mice analysed.

Site	*Ni*	*Nsh*	2*n*	3.8	4.14	5.15	6.10	7.17	9.11	12.13
Ametlla de Segarra	1	16	39	A	H	A	A	A	A	A
	1	20	39	A	H	A	A	A	A	A
Arbeca	2	18	40	A	A	A	A	A	A	A
Badalona	5	19–20	40	A	A	A	A	A	A	A
	1	20	39	A	A	A	A	A	A	H
Cubelles	1	20	37	A	H	A	A	A	H	H
	1	20	34	A	H	H	A	A	M	M
	1	20	34	A	H	M	A	A	M	H
El Prat de Llobregat	1	19	33	A	H	H	H	A	M	M
	1	20	35	A	H	M	A	A	H	H
	1	19	34	A	A	M	A	A	M	M
	1	16	32	A	M	H	H	A	M	M
	1	20	31	A	M	M	M	A	H	M
Gavà	1	20	30	M	M	M	H	A	H	M
	1	20	32	A	M	M	H	A	H	M
	1	21	30	H	M	M	H	A	M	M
	1	20	33	A	M	H	H	A	H	M
Sant Martí Sarroca	1	20	34	A	M	A	A	A	M	M
	1	15	32	A	M	M	A	A	M	M
	1	18	32	A	M	H	A	H	M	M
Sta. Perpètua de la Mogoda	6	20	40	A	A	A	A	A	A	A
Viladecans	1	20	31	M	M	H	H	A	M	H

552 **Table 2.** Mahalanobis distances between chromosomal groups.

	Rb(30–32)	Rb(33–37)	Rb(38–40)
Rb(33–37)	1.4165*		
Rb(38–40)	2.0790*	1.7270*	
Rb(40 St)	3.2486*	3.2133*	3.2857*

557

558 *$P < 0.001$.

Table 3. Probabilities for Tukey's post-hoc test on centroid size relative to diploid number (2*n*) and the structural composition of the karyotype (Ht).

	St AA	Rb(38–40) AA	Rb(38–40) Ht	Rb(33–37) Ht	Rb(33–37) MM	Rb(30–32) Ht	Rb(30–32) MM
St AA	–	0.192	1	0.382	0.098	0.001*	0.019*
Rb(38–40) AA	–	–	0.422	0.001*	0.001*	0.600	0.001*
Rb(38–40) Ht	–	–	–	0.788	0.276	0.007*	0.048*
Rb(33–37) Ht	–	–	–	–	0.853	0.001*	0.237
Rb(33–37) MM	–	–	–	–	–	0.001*	0.859
Rb(30–32) Ht	–	–	–	–	–	–	0.001*
Rb(30–32) MM	–	–	–	–	–	–	–

AA, individuals with all acrocentric chromosomes; Ht, specimens with between one and three heterozygous fusions; and MM, mice with homozygous fusions only.

*$P < 0.05$.

Figure legends

Figure 1. A, light microscopy (LM) image. B, scanning electron microscopy (SEM) image. C, diagram of the sperm head features and location of the 16 landmarks (points 1–15 and 19) and three semilandmarks (points 16–18) in the sperm head of *Mus musculus domesticus*; AA, anterior acrosomal region; ES, equatorial segment; P, perforatorium; PAS, postacrosomal sheath; VS, ventral spurs. Landmark assignation: 1, top of the hook; 2, point where the hook and the upper ventral spur overlap; 3, prominence in the axis of the upper ventral spur; 4 and 7, tops of the upper and lower ventral spurs, respectively; 5 and 6, inner distance between the ventral spurs; 8–11, insertion edge of the sperm head with flagellum; 12 and 13, terminal edges of the post-acrosomal sheath; 14, 15, and 19, basal and apical ridge of the equatorial crest; 16–18, semilandmarks around the curved contour of the anterior acrosomal region.

Figure 2. Biplot of the individual scores onto the first two canonical variate axes according to diploid number.

Figure 3. Deformation grids and landmark variation along the first (CV1) and second (CV2) canonical axes. The positive is assumed as the reference shape configuration.

Figure 4. Variation of the sperm head shape scores (mean ± SE) of the first (CV1) and second (CV2) canonical axes with reference to the diploid number and structural composition of the karyotype.

Figure 5. Variation of the centroid size (CS; mean ± SE) of the sperm head in relation to the diploid number and the structural composition of the karyotype.

SUPPORTING INFORMATION

Appendix S1. Comparison of the sperm head measurements obtained from Rb(30–32) and Rb(38–40) mice by light microscopy (LM) and scanning electron microscopy (SEM) techniques. SHL, sperm head length; SHW, sperm head width.

Appendix S2. Linear (left) and Passing–Bablok (right) regression analyses of width and length of the sperm head between light microscopy (LM) and scanning electron microscopy (SEM) techniques. CI, confidence interval.

Appendix S3. Biplot of the individual scores onto the first two canonical variate axes according to the structural composition of the karyotype. AA, individuals with all acrocentric chromosomes; Ht, specimens with between one and three heterozygous fusions; and MM, mice with homozygous fusions only.

Figure 1

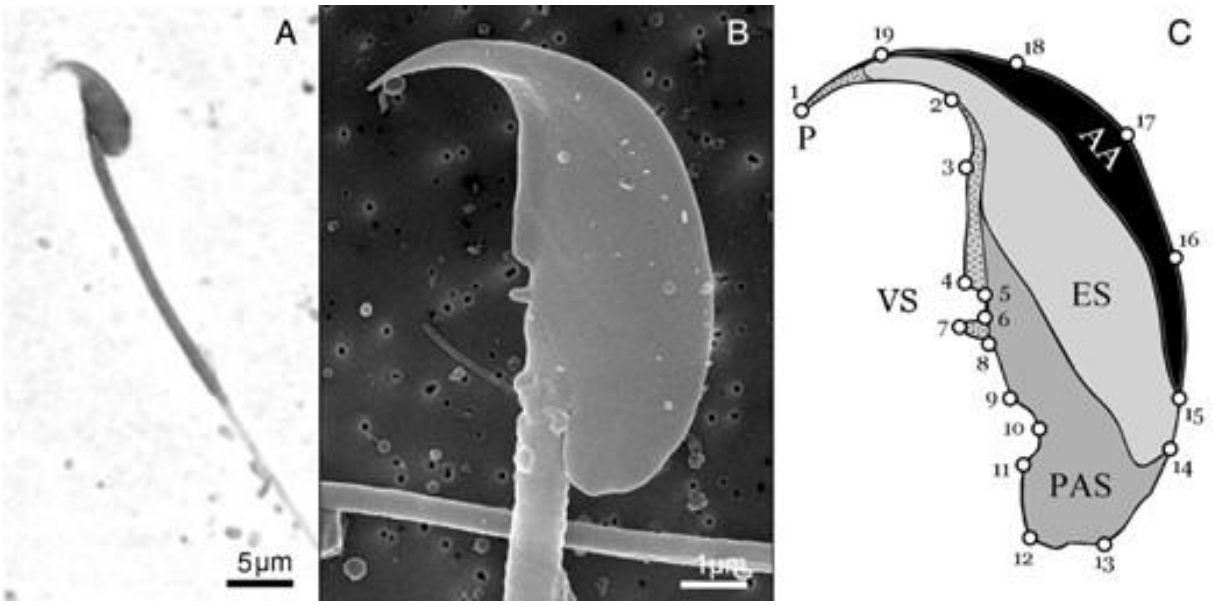

607 **Figure 2**

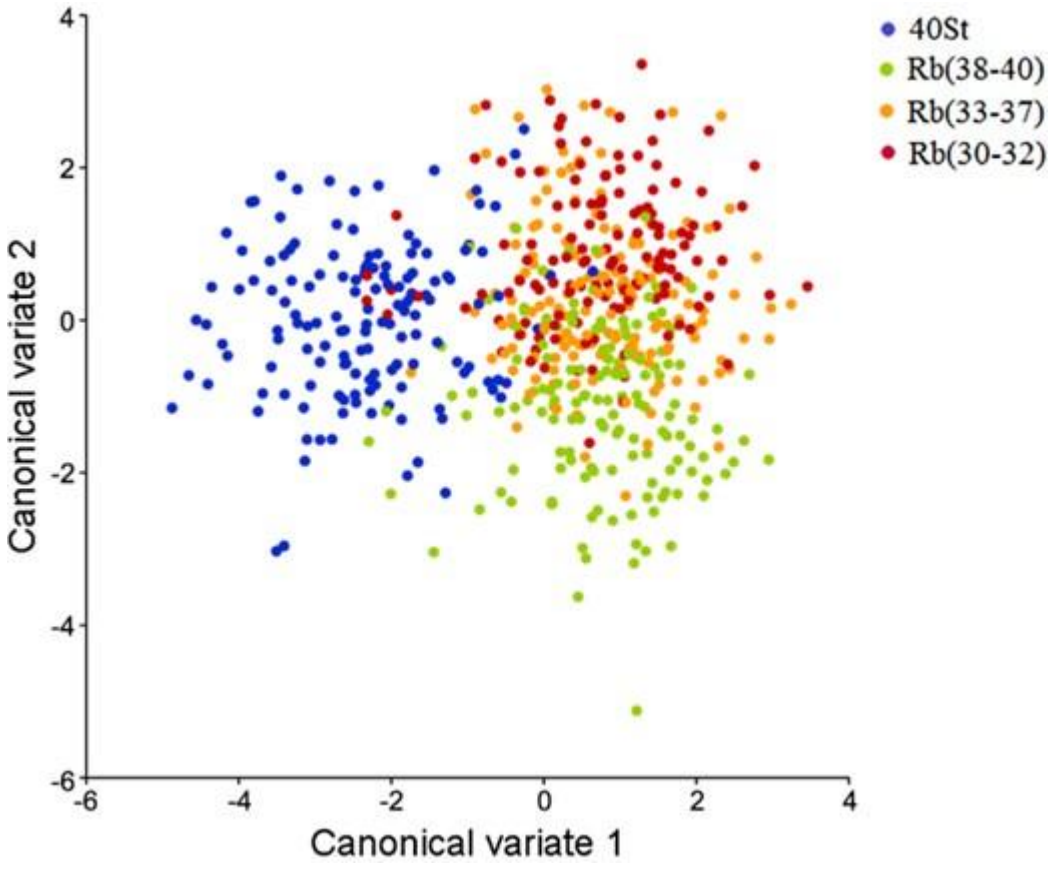

608

609 **Figure 3**

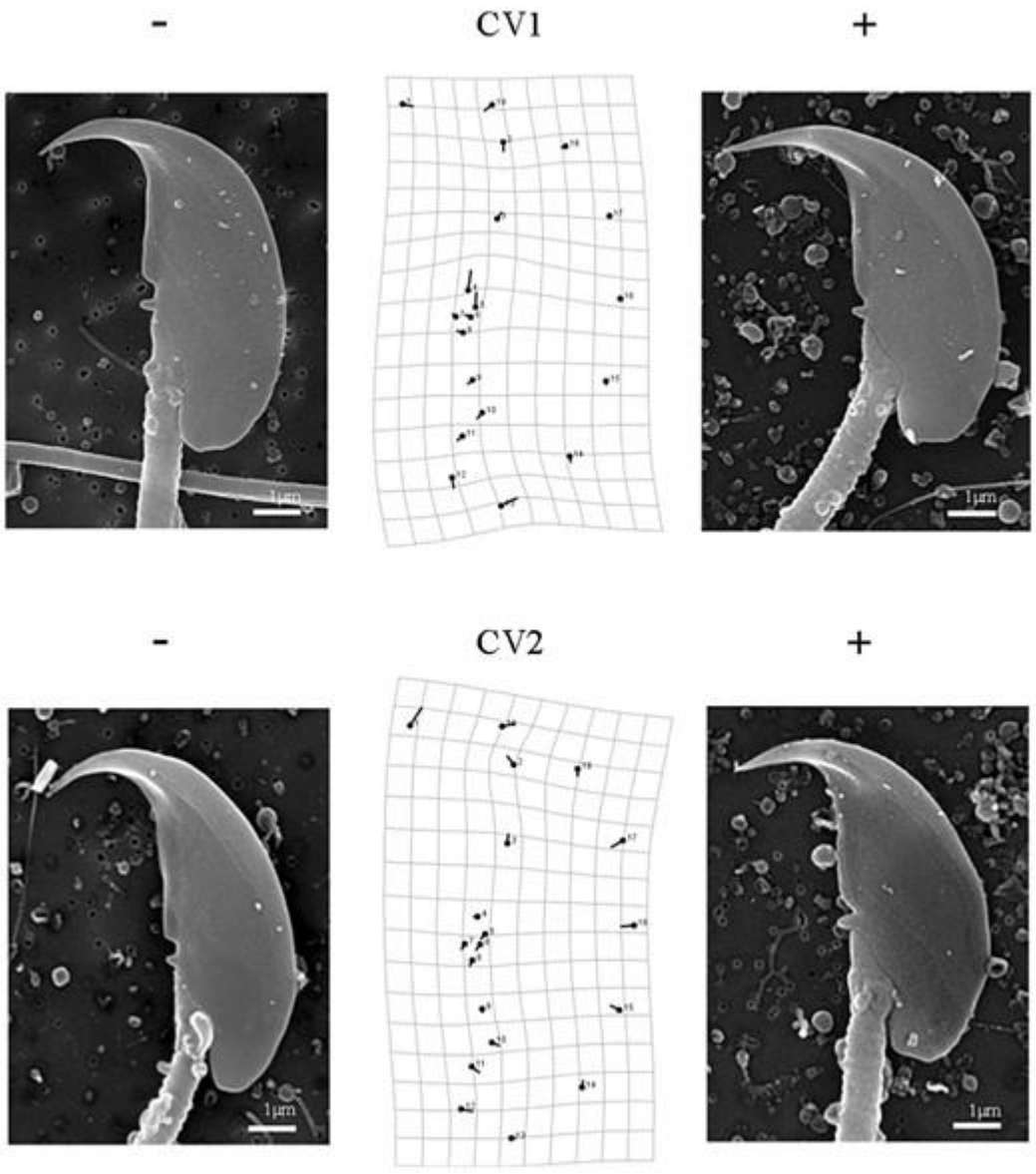

610

611 **Figure 4**

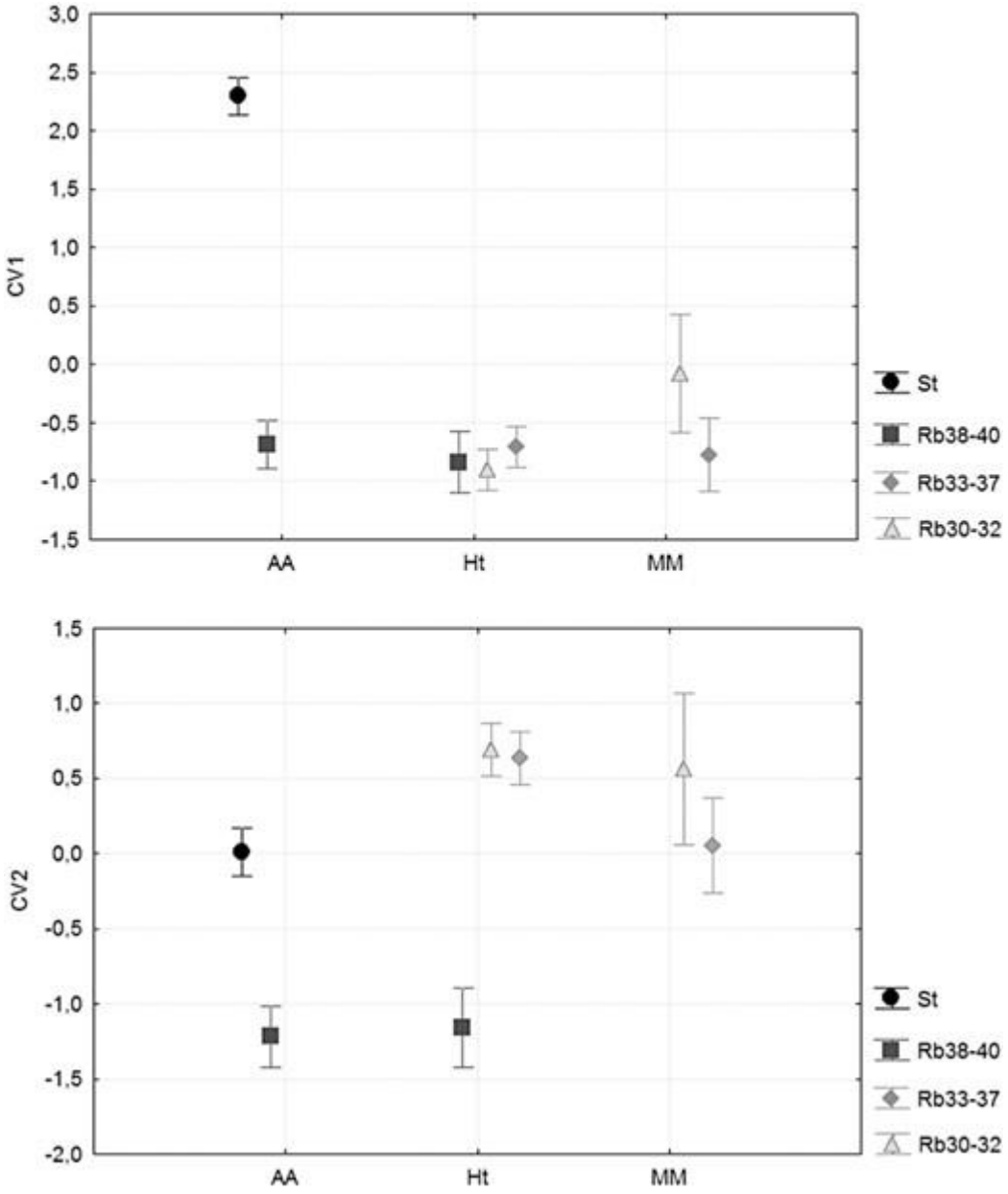

612

613 **Figure 5**

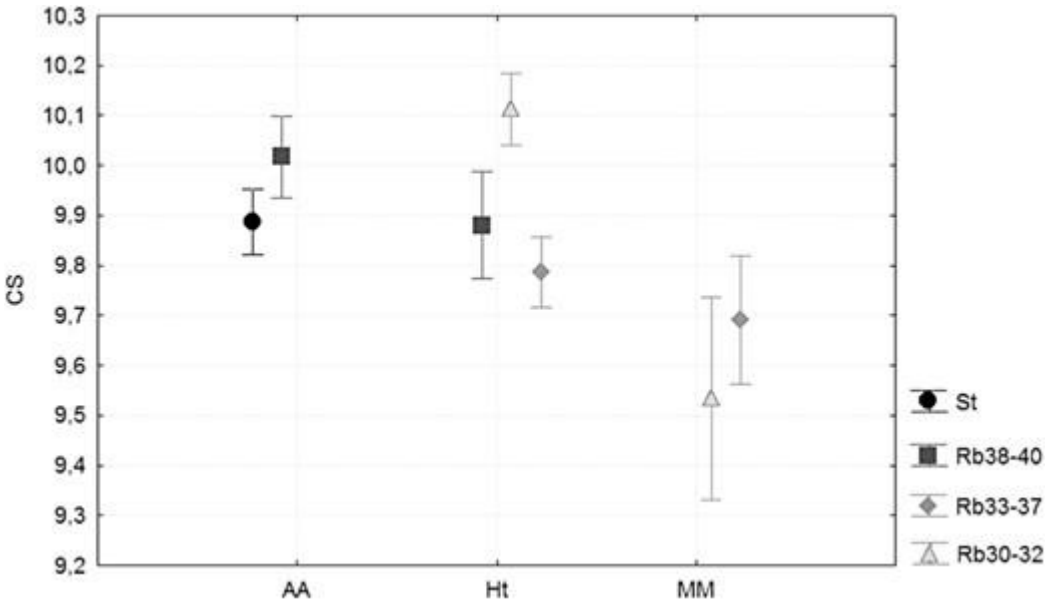

614

615

616 **Appendix S1**

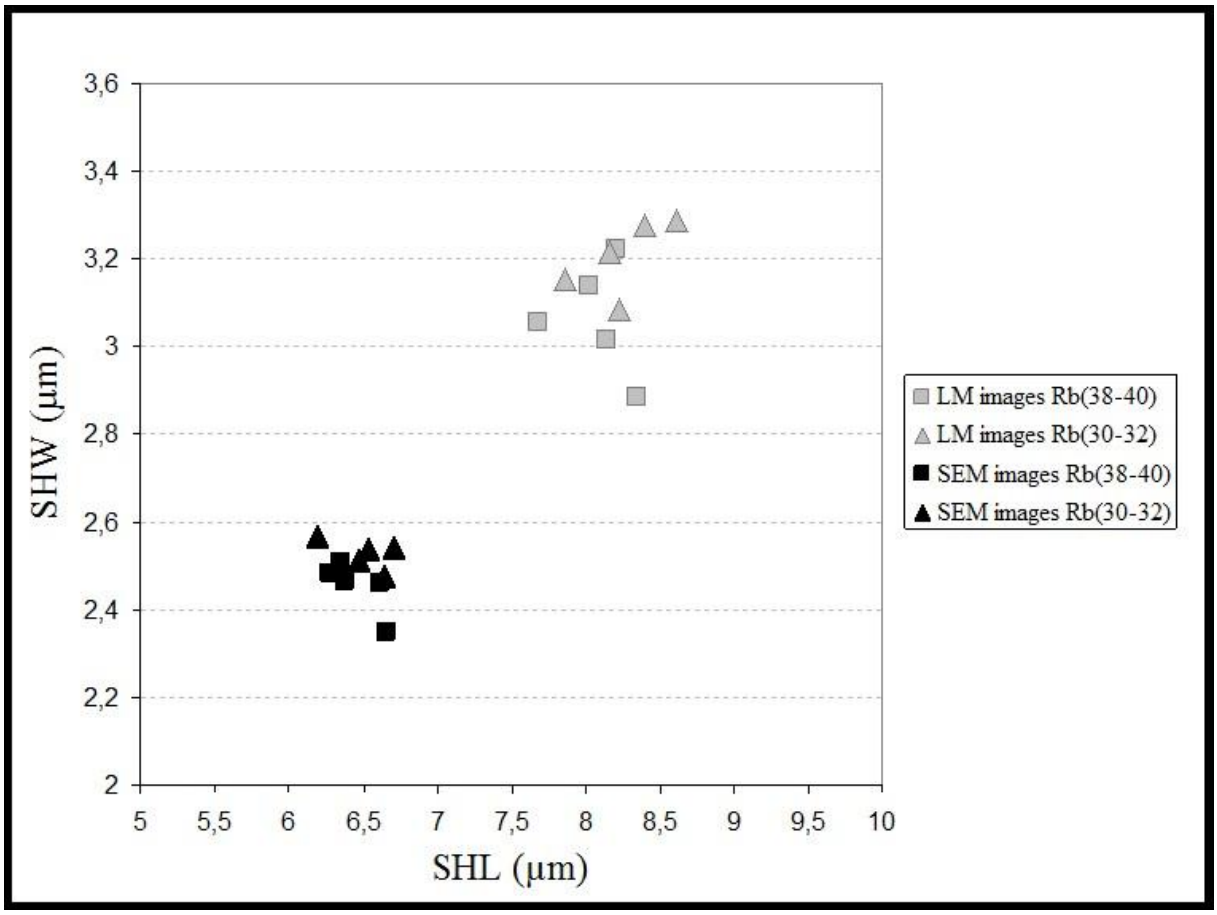

617

618 **Appendix S2**

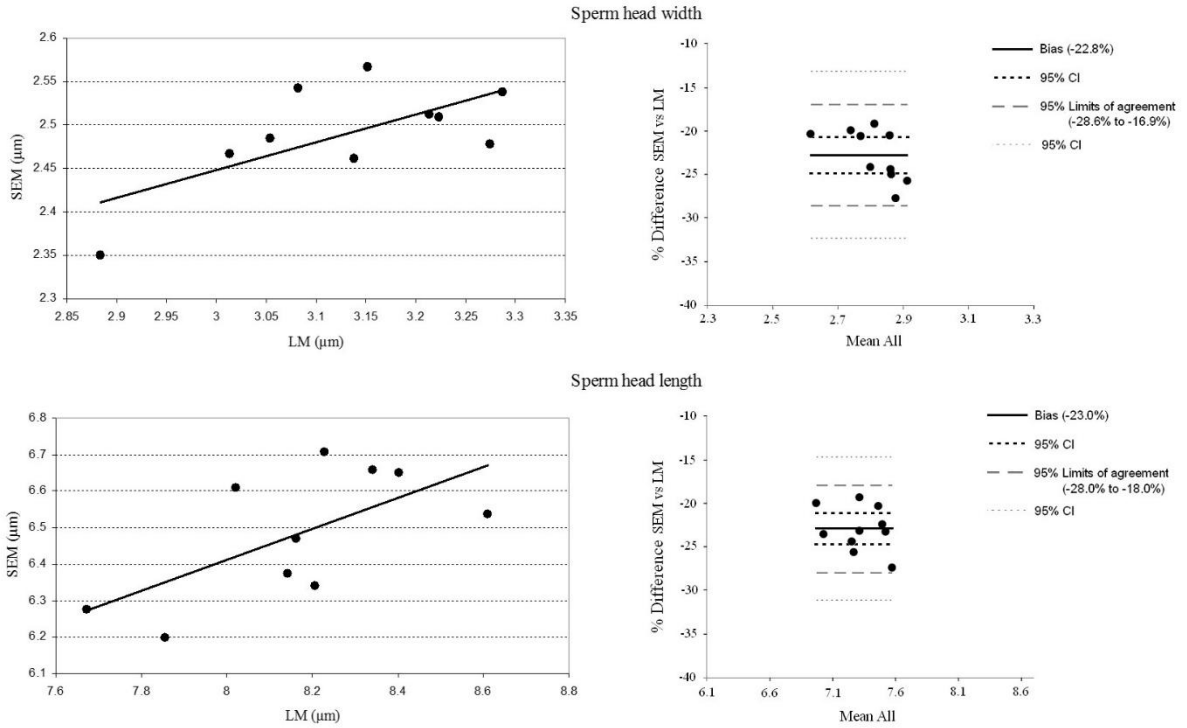

619

620 **Appendix S3**

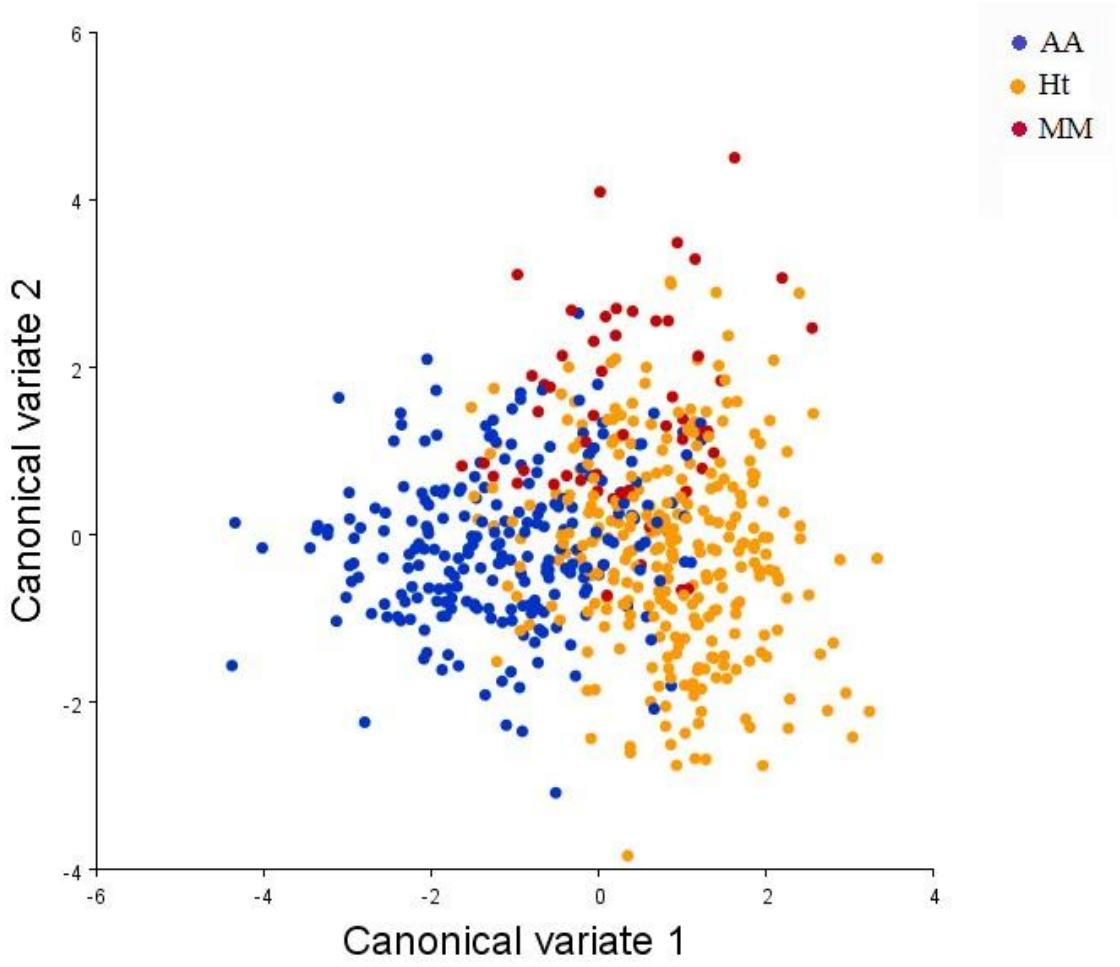

621